



NMR of a single nuclear spin detected by a scanning tunnelling microscope

Yishay Manassen^a, Michael Averbukh^a, Zion Hazan^a, Yahel Tzuril^a, Pino Boscolo^b, Alexander Shnirman^c, Baruch Horovitz^{a,*}

^a Department of Physics, Ben Gurion University of the Negev, Beer Sheva 84105, Israel

^b Gruppo Tecniche Avanzate, Via Vergerio 1, 34138 Trieste, Italy

^c Institut für Theorie der Kondensierten Materie, Karlsruhe Institute of Technology, D-76131 Karlsruhe, Germany

ARTICLE INFO

Keywords:

Single molecule NMR

Scanning tunnelling microscope

Chemical shifts

ABSTRACT

We detect a single spin nuclear magnetic resonance (NMR) by monitoring the intensity modulations of a selected hyperfine line in the electron spin resonance (ESR) spectrum. We analyse the power spectrum of the corresponding hyperfine intensity and obtain the nuclear magnetic resonance (NMR) spectrum. Our process also demonstrates ionization of a molecule with the bias voltage of a Scanning Tunnelling Microscope (STM), allowing detection of NMR even in molecules that are non-radical in their neutral state. We have observed this phenomenon in four types of molecules: toluene, triphenylphosphine, TEMPO and adenosine triphosphate (ATP) showing NMR of ^1H , ^{13}C , ^{31}P and ^{14}N nuclei. The spectra are detailed and show signatures of the chemical environment, i.e. chemical shifts. A theoretical model to account for these data is outlined.

The detection of Nuclear Magnetic Resonance (NMR) of individual molecules is an outstanding challenge. Single-spin NMR enables methods in chemical analysis, quantum information, and medical NMR. Previous attempts to probe local NMR by magnetic resonance force microscopy [1,2] have reached a resolution of 10 nm by using NV centers [3–5], however, this method lacks the flexibility of sample scanning. Further attempts used optical double resonance methods [6] to detect NMR of labelled molecules or in conjunction with STM [7], these methods yielded a rather poor linewidth of ~ 30 KHz.

We have previously developed a technique for measuring electron-spin-resonance (ESR) known as ESR-STM [7–9]. In contrast with other ESR-STM methods [10,11] our scheme requires neither a polarized STM tip, nor high magnetic fields, nor low temperatures, nor even external rf fields. Therefore, our method has the advantage of simplicity.

In the present work, while we make use of our ESR-STM technique [7–9], we present a major modification to that technique by developing an ionization process in conjunction with a real time method of analysis. This method yields the NMR spectra of nuclei in a single molecule to an accuracy of a few Hz with a linewidth of ~ 10 Hz. This accuracy allows detection of chemical shifts [12], providing identification of the chemical environment of nuclei and thus detecting their molecular fingerprints. Combined with the STM scanning capability and spatial resolution of ~ 1 nm, our method is by far superior to previous methods for single molecule NMR [1–7].

1. Principles and outline

The present work can be applied to either radical or non-radical molecules. In the radical state the hyperfine tensor couples the electron and nuclear spins, hence a nuclear spin rotation can modulate the intensity of a hyperfine line, which in turn is detectable in ESR-STM. Furthermore, the STM bias ionizes the molecules, as evident in the non-radical case, hence we expect in all cases a coexistence of neutral and ionic states. The challenge is then, both experimentally and theoretically, to create conditions where a free nucleus encodes its precession phase on the ESR spectrum.

In our experiments we probe various nuclei such as ^1H , ^{13}C , ^{31}P and ^{14}N . The STM bias voltage is modulated in time between low and high values so as to enhance ionization, the signal is, however, present even without modulation though with lower intensity. We then record a given hyperfine intensity during a sequence of dwell times, each one is short relative to the nuclear period. Finally we identify the power spectrum of this sequence as our NMR spectrum. We find that in 1 s we can take an NMR spectrum of each pixel in an STM image. Our experiments are then a proof of concept, providing a powerful yet simple technique for detection of single nucleus NMR. Furthermore, the NMR spectrum with high frequency resolution provides chemical shifts [12] and spin–spin (dipolar) interactions, hence the chemical environment of the nucleus.

* Corresponding author.

E-mail address: hbaruch@bgu.ac.il (B. Horovitz).

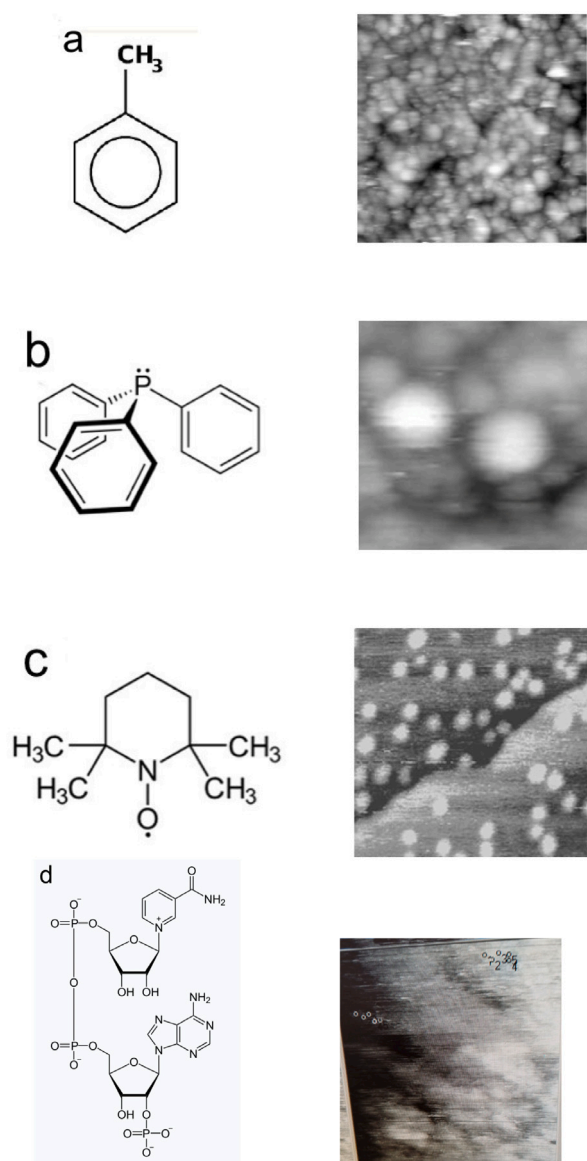


Fig. 1. Molecular structures and STM images. Left: atomic structure of molecules, right: their STM image on Au(111) substrate ($20 \times 20 \text{ nm}^2$ for a, c, d, $10 \times 10 \text{ nm}^2$ for b). STM current is $I = 0.1 \text{ nA}$ and voltage 1 V . (a) toluene, (b) triphenylphosphine, (c) TEMPO covered with graphene oxide monolayer, (d) Adenosine triphosphate (small circles on the image indicate STM locations where data was taken).

We demonstrate our technique on four types of molecules: toluene molecules that are non-radicals at zero bias and become radicals in the ionized state, triphenylphosphine, (2,2,6,6-Tetramethylpiperidin-1-yl)oxyl (TEMPO) and adenosine triphosphate (ATP), which are radicals at zero bias and becomes non-radicals in their ionized state, see structures and STM images in Fig. 1. We note also recent experiments [13] on ^{60}Co which is non-radical at zero bias, becoming a radical at finite STM bias as seen by its ESR-STM spectrum. In the last section a theoretical model to account for these data is outlined.

2. NMR-STM experiments

Consider first our NMR-STM experiments on toluene, identifying ^1H nuclei. This molecule is significant as it demonstrates that the non-magnetic toluene in its neutral state becomes paramagnetic in its ionized state, enabling the observation of NMR. ESR-STM data is shown in the appendix, Fig. 7. We have chosen the ESR intensity at

627 MHz and recorded its value during $0.5 \mu\text{s}$ (dwell time T_d) by a fast oscilloscope (Rhode Schwarz) taking $2 \cdot 10^6$ values, i.e. a total acquisition time of 1 s . This set of ESR intensities forms a sequence $h(t)$ (proportional to the ESR intensity in dBm units) at times t separated by T_d . The corresponding Fourier spectrum $|h(\nu)|^2$ representing the NMR spectrum is then plotted. The nominal magnetic field at the beginning of the experiment was $B = 230 \text{ G}$ though it was not monitored during the experiment. We have examined over 100 spectra, all having a sharp line near the expected position of the ^1H NMR. A typical NMR spectrum is shown on the whole frequency range in Fig. 2a, the vertical scale is chosen to exhibit the background noise, hence just 4% of the ^1H resonance intensity is shown. The resonance at 0.96486 MHz is shown with full vertical scale in Fig. 2b, the signal to noise ratio near the resonance is ≈ 1000 . We also show in Fig. 2c five consecutive spectra over a given molecule (including the one in Fig. 2b), showing line positions that vary by $\sim 0.1\%$, possibly due to a slight drift of either the magnetic field or the tip position. The gyromagnetic value of ^1H 42.577 MHz/T implies that the actual field is 226.6 G .

The recorded $2 \cdot 10^6$ points allow detection of chemical shifts. This is shown in the very high resolution Fig. 2d that shows splitting of $\sim 10 \text{ ppm}$, as in standard data [14] and also within the range of dipole-dipole interactions [15]; in this figure the data has been smoothed to avoid the inherent discreteness of 1 Hz . Fig. 2e shows data at a different site at a higher magnetic field, it shows splittings of $\sim 100 \text{ ppm}$, possibly stronger chemical shifts. This demonstrates that the resonance position indeed shifts in proportion with the magnetic field, within the latter's accuracy. We emphasize that our NMR linewidth is orders of magnitude smaller than that of the ESR, the latter is $\sim 10 \text{ MHz}$. We note that the NMR frequency and linewidth are actually maintained if we were to monitor instead of 627 MHz a different ESR frequency within the ESR linewidth.

We consider next our data on triphenylphosphine molecules in Fig. 3 showing resonances of ^{13}C , ^{31}P and ^1H . Spectra were taken in groups of 50, repeated 4 times. Fig. 3a shows the full spectrum with dashed lines indicating the expected resonances at $B = 225 \text{ G}$, using the gyromagnetic factors 10.7084 MHz/T of ^{13}C , 17.235 MHz/T of ^{31}P and 42.577 MHz/T of ^1H ; we note deviations of up to $\sim 4\%$. We also note that the 1.1% natural abundance of ^{13}C is compensated by the presence of 18 C atoms in this molecule. In Figs. 3c, 3d, 3e we show high resolution data of summed 50 spectra as well as individual spectra (in red). The individual spectra show more refined chemical shifts. In particular the triplet of ^{31}P with splitting of 20 Hz is consistent with chemical shifts in similar molecules [16].

We present in Fig. 3 further data on triphenylphosphine at a higher nominal magnetic field of $B = 300 \text{ G}$. Spectra were taken in groups of 100, repeated 15 times, 7 of which exhibit sharp lines as in Fig. 3b. This data shows the lines of ^{13}C and of ^{31}P shifted to higher frequencies (compare Figs. 3a, 3b) corresponding to the increased magnetic field. We note a 3rd line in Fig. 3b that corresponds exactly (to accuracy of 5 Hz , within the linewidth) to the sum of the observed lines of ^{13}C and ^{31}P . This harmonic is seen here in view of the improved frequency resolution. The ^1H line is not observed, we propose that monitoring different ESR frequencies (e.g. compare Figs. 3a and 3b) selects different hyperfine lines for the real time analysis which in turn probe different nuclei. In Figs. 3f, 3g we show high resolution data of the summation over 100 spectra, chemical shifts are therefore barely visible.

Consider next our NMR-STM experiment on TEMPO and ATP molecules focusing on ^{14}N . This nucleus is of special significance in view of its high natural abundance and its prevalence in organic and biological systems. ^{14}N is a spin 1 nucleus with a quadrupole interaction, its strength is usually $1\text{--}5 \text{ MHz}$ [17,18], however it was not measured in either TEMPO or ATP. The detection of this quadrupole moment, even in the bulk, is challenging and has lead to a number of experimental techniques [19].

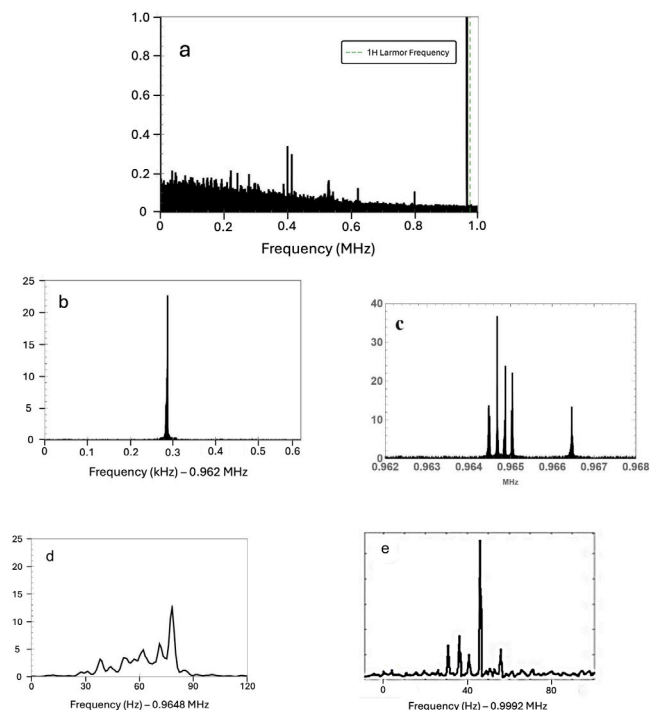


Fig. 2. Data on toluene. (a) Single nucleus NMR of ^1H in toluene, the signal near 0.97 MHz is shown with just 4% of its intensity. The scale is chosen so as to exhibit the background noise. A dashed line indicates the expected resonance for the nominal $B = 230$ G. (b) Full size of the signal in (a). (c) Five consecutive measurements, including the one shown in (b). (d) A high resolution spectrum of the signal in (b) showing chemical shifts between aromatic and aliphatic hydrogen peaks. Voltage modulation is between 0.2 V and 3.7 V at a frequency of 15.675 MHz, $I = 0.1$ nA, $T_d = 0.25$ μs . (e) Same parameters except $B = 235$ G, demonstrating that the NMR peak indeed shifts with B .

ESR data on TEMPO using our ESR-STM method was presented with various TEMPO configurations [20]. We have chosen the ESR intensity at 760 MHz and recorded its value during $T_d = 0.25$ μs , taking 10^6 values, i.e. total of 0.25 s. We have taken 50 spectra within 5 min forming one group, then searched the STM image for another molecule and repeated this procedure, thus generating 101 groups, the nominal magnetic field was $B = 233$ G. Fig. 4a shows the full range of the spectrum, summing on the 50 spectra of one group. A strong line is visible at 0.0785 MHz and is present in about 1/3 of the groups, which we relate to ^{14}N . A high resolution plot is shown in Fig. 4b of the sum on 50 spectra as well as that of one individual spectrum. The linewidth is ~ 100 Hz, as common in molecules with ^{14}N [17]. The individual spectrum exhibits considerable structure, consistent with known chemical shifts [17]. There are two weaker lines at 0.2303 MHz, which is likely to be a ^{13}C NMR, and a 1.544 MHz line that might be extrinsic noise. The ^1H signal is absent, as in the triphenylphosphine case its presence depends on which ESR frequency is monitored.

To interpret the TEMPO data we note that the standard gyromagnetic ratio of ^{14}N is $\gamma_N = 3.0717$ MHz/T, hence $\gamma_N B = 0.072$ MHz is fairly close to the observed line at 0.0785 MHz. Thus our first interpretation is that the quadrupole effect is relatively weak and amounts to a small shift in the NMR frequency. This is supported by the ATP data (Fig. 5 below) that also shows a resonance at a very similar frequency.

We propose a second interpretation, in case that the quadrupole effect is significant. We recall that the eigenstates of nuclear spin 1 in a quadrupole field, in its principal axis system, are characterized by a frequency parameter K and an anisotropy parameter $0 \leq \eta \leq 1$. In terms of the spin angular momenta the eigenvectors are $[|1\rangle \pm |-1\rangle]/\sqrt{2}$ with eigenvalues $K(1 \pm \eta)$ and $|0\rangle$ with eigenvalue $-2K$. Assuming that

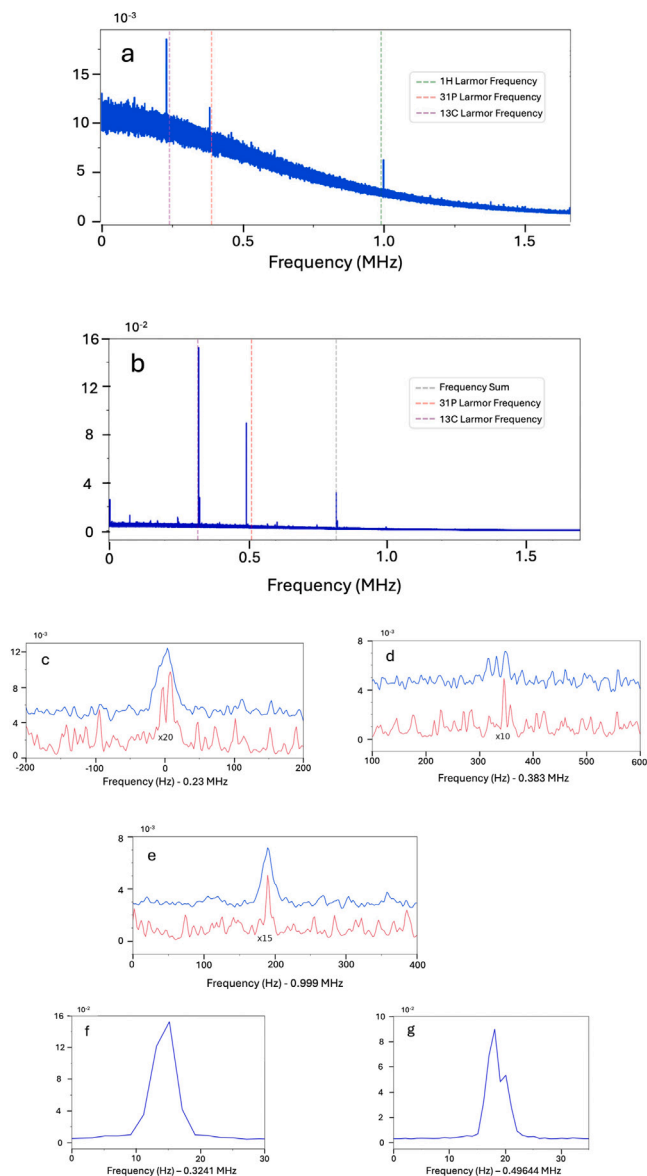


Fig. 3. Data on triphenylphosphine. NMR data showing multiple isotope lines and the magnetic field effect. (a) Monitored ESR frequency is 734 MHz, voltage is modulated between 0.2 V and 3.8 V at 16.5 MHz, $I = 0.5$ nA, $T_d = 0.25$ μs , data is averaged over 50 consecutive spectra. Dashed lines indicate the expected resonances for the nominal $B = 225$ G. (b) Monitored ESR frequency is 620 MHz, voltage modulation is same as in (a), $I = 0.2$ nA, $T_d = 1/6$ μs . Dashed lines correspond to the nominal $B = 300$ G. Data is averaged over 100 consecutive spectra. Data of (a) is shown with high resolution for the ^{13}C line (c), the ^{31}P line (d) and the ^1H line (e). The lower lines in red (4c, 4d, 4e) show individual spectra, enhanced as indicated. Data of (b) is shown with high resolution for the ^{13}C line (f) and the ^{31}P line (g).

$K \gg \gamma_N B$ and that $\eta \ll 1$, the dominant contribution of the magnetic field is $\gamma_N H \cos \theta$ where θ is the angle between the external magnetic field and the z axis of the quadrupole. The latter term is off-diagonal in the subspace of the almost degenerate eigenvalues $K(1 \pm \eta)$. The difference of the two dipole allowed frequencies is then

$$\nu_0 = 2\sqrt{(\gamma_N H \cos \theta)^2 + (\eta K)^2} + O(\gamma^2 K, \gamma_N^2 H^2 / K) \quad (1)$$

We propose that our observed frequency is the interference ν_0 between the dipole allowed frequencies. We have monitored such interference also in the data of triphenylphosphine (Fig. 3b). With the value of $\gamma_N B = 0.072$ MHz, we obtain $\theta > 57^\circ$. By extending our data to higher

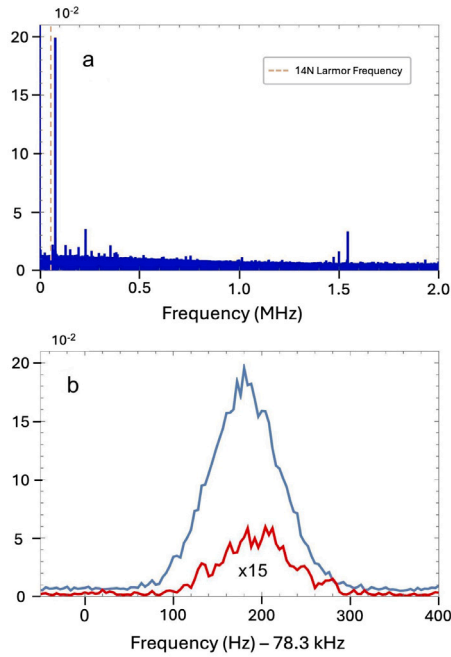


Fig. 4. Data on TEMPO. (a, b) NMR spectrum with monitored ESR frequency of 760 MHz, voltage is modulated between 0.2 V and 3.8 V at 15 MHz, tunnelling current is $I = 0.5$ nA, $T_d = 0.25$ μ s, a dashed line indicates the NMR position $\gamma_N B$ in the absence of a quadrupole moment. Data is summed over 50 consecutive spectra while (b) shows also a single spectrum (lower red line, enhanced by x15).

frequencies the NMR-STM technique can distinguish between the two interpretations and would determine the quadrupole parameters.

We finally present our data on ATP, a molecule of exceptional biological significance. We have taken 440 NMR spectra, 25 of which show sharp signals as shown in Fig. 5a, i.e. lines at 0.07136 MHz, 0.25 MHz and 0.32 MHz. For our field of 230 G with the preceding gyromagnetic ratios we obtain 0.071 MHz for ^{14}N , 0.246 MHz for ^{13}C and 0.396 MHz for ^{31}P . The 0.32 MHz line is somewhat off the expected position for ^{31}P , we suggest then that this is a frequency sum of the two other resonances. In this case both ^{31}P and ^1H are not seen, as noted above the observed NMR lines depend on which ESR frequency is being monitored. The 0.07 MHz line is shown with high resolution in Fig. 5b. The closeness of this resonance to $\gamma_N B$ implies that the quadrupole effect is either negligible or that the anisotropy η in Eq. (1) is small, as in the case of TEMPO.

3. Theoretical model

We outline here a model that has two scenarios (at least), depending on parameters, that account for a sharp NMR line as seen in the data. The details are in a separate publication [21]. We note first that an off-diagonal hyperfine element is essential for observing the NMR signature, i.e., the minimal nuclear part of the Hamiltonian is

$$H_n = \frac{1}{2} v_n \tau_z + a \sigma_z \tau_z + d \sigma_z \tau_y, \quad (2)$$

where τ , σ are Pauli matrices for the nuclear and electron spins, respectively, v_n is the nuclear precession frequency in a z oriented magnetic field, and a , d are hyperfine couplings. It is known [22] that a rotated molecule has in general a such an off-diagonal term, i.e., $d \neq 0$.

We express the hyperfine term as $\tilde{a} \sigma_z \tilde{\tau}$, where $\tilde{a} = \sqrt{a^2 + d^2}$ and $\tilde{\tau} = (a \tau_z + d \tau_y) / \sqrt{a^2 + d^2}$. We observe that $\tilde{\tau}$ is the nuclear spin component responsible for the hyperfine shift of the ESR resonance. If it is made to oscillate slowly, e.g., with the frequency close to v_n , the ESR intensity would oscillate accordingly.

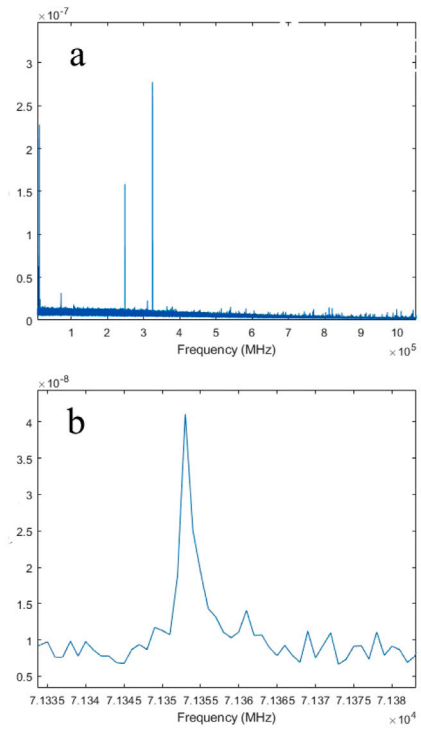


Fig. 5. Data on adenosine triphosphate (ATP). ESR is monitored at 620 MHz, the other parameters are as in Fig. 2. Data is at full frequency scale (a) and with high resolution in (b).

The simplest scenario is when the electronic spin polarization σ_z fluctuates on a time scale much faster than v_n and averages almost to zero. This scenario, akin to the motional narrowing, allows for a sharp NMR resonance. It requires $\gamma_1 \gg \tilde{a}$, where γ_1 is the longitudinal relaxation rate of the electronic spin (related to the ESR line width). More specifically, the time evolution of the nuclear raising operator $\tilde{\tau}_+$ (that describes the nuclear spin precession), neglecting here v_n , is given by

$$\begin{aligned} \tilde{\tau}_+(t) &= e^{-i\tilde{a}\tilde{\tau} \int_0^t \sigma_z(t') dt'} \tilde{\tau}_+ e^{i\tilde{a}\tilde{\tau} \int_0^t \sigma_z(t') dt'} = e^{-2i\tilde{a} \int_0^t \sigma_z(t') dt'} \tilde{\tau}_+ \\ \Rightarrow \langle \tilde{\tau}_+(t) \rangle &\sim \langle e^{-2i\tilde{a} \int_0^t \sigma_z(t') dt'} \rangle = e^{-\frac{2\tilde{a}^2}{\gamma_1} t} \end{aligned} \quad (3)$$

where the σ_z correlation at zero frequency is given by $1/\gamma_1$. If v_n is taken into account, $d \neq 0$, and the dephasing rate $2\tilde{a}^2/\gamma_1 \ll v_n$ (motional narrowing), we expect $\tilde{\tau}$ to perform slowly decaying oscillations with frequency close to v_n . This is exactly what is detected in the ESR signal.

We note that the nucleus feels an additional effective magnetic field $\tilde{a}\langle\sigma_z\rangle$ if the electron spin is polarized. However, under an STM bias V the electron spin occupation are determined [23] by eV rather than temperature T , since $eV \gg k_B T$. Hence the spin polarization $\langle\sigma_z\rangle$ vanishes to a very high accuracy.

In some experimental cases the ESR hyperfine lines are resolved so that actually $\tilde{a} > \gamma_1$. We propose then that there are two nuclei with the same v_n , one of them has $\tilde{a} > \gamma_1$ consisted with the ESR data, while the other nucleus has $\tilde{a} \ll \gamma_1$. This second nucleus is not visible in the ESR, yet it allows its NMR to be seen. This situation is manifest in the toluene case that has many ^1H sites with varying hyperfine couplings [24].

In our second scenario we allow the presence of a second molecule that collects the electron which is being ionized. A second radical is actually essential for observing ESR-STM [23]. We label as $|11\rangle$ the subspace where the two electron spins are on separate molecules while one of the spins is hyperfine coupled with a nuclear spin $\frac{1}{2}$. In addition, we have the subspace where both spins are on the same molecule in a singlet state, labelled as $|20\rangle$. We aim to find a situation where the free

nuclear spin rotation within the $|20\rangle$ state is weakly dephased while in the $|11\rangle$ state. We note that in general the $|11\rangle$ and $|20\rangle$ states coexist coherently or partly incoherently in view of dissipative transitions of strength γ between them. While their relative weight may oscillate in response to the STM voltage modulation these states coexist even without such modulation. Within our master equation [21] we find that a sharp NMR resonance is indeed possible if γ is large while γ_1 is small. We find that the resonance position does not shift even if we allow a finite electron spin polarization, i.e. the NMR resonance is indeed generated in the $|20\rangle$ state. Further experimental data are needed to identify γ and the presence of a second molecule.

4. Conclusions

In conclusion, our work demonstrates the successful observation of single spin NMR, a proof of concept which is detected experimentally and supported theoretically. We note that a clear single spin NMR spectrum can be achieved within 1 s, close to the time that a (slow) scan of STM takes to record 1 pixel. This opens the road for observing an atomically resolved STM image concurrently with identifying each nucleus

CRediT authorship contribution statement

Yishay Manassen: Project administration, Methodology, Investigation, Data curation. **Michael Averbukh:** Software, Resources. **Zion Hazan:** Investigation, Data curation. **Yahel Tzuril:** Investigation, Data curation. **Pino Boscolo:** Methodology. **Alexander Shnirman:** Software, Investigation. **Baruch Horovitz:** Methodology, Investigation.

Declaration of competing interest

The authors declare the following financial interests/personal relationships which may be considered as potential competing interests: Yishay Manassen reports financial support was provided by EIC grant 101099676. If there are other authors, they declare that they have no known competing financial interests or personal relationships that could have appeared to influence the work reported in this paper.

Acknowledgements

This work was funded by the attract grant “NMR(1)”, Israel. Additional funding was provided by the ISF – collaboration with China “ESR-STM study of individual radical ions at the single molecule level”, the DFG project “Magnetism of Vacancies and edge states in graphene probed by electron spin resonance and scanning tunnelling spectroscopy” and by the EIC grant, Israel 101099676 “Single Molecule Nuclear Magnetic Resonance Microscopy for Complex Spin Systems”.

Appendix A. Materials and methods

In this appendix we provide some technical details of our setup and also present two additional methods of data analysis.

Our experiments were carried out with a Demuth type STM operated at room temperature in ultrahigh vacuum (UHV) (base pressure $\leq 1.5 \cdot 10^{-10}$ Torr). STM images were acquired with chemically etched tungsten tip (W). The molecules were deposited on gold films of thickness 100 nm on Mica. The deposition was done in two ways: TEMPO was dissolved in toluene and drop casted on the surface at a concentration of 0.041 g/25 ml, corresponding to one monolayer. Toluene and triphenylphosphine were evaporated for few minutes with a leak valve maintaining base pressure of 10^{-8} Torr in the chamber. Molecular resolution was achieved, and it was easy to identify single molecules on the surface (Fig. 1). The next step was to study their magnetic resonance signature.

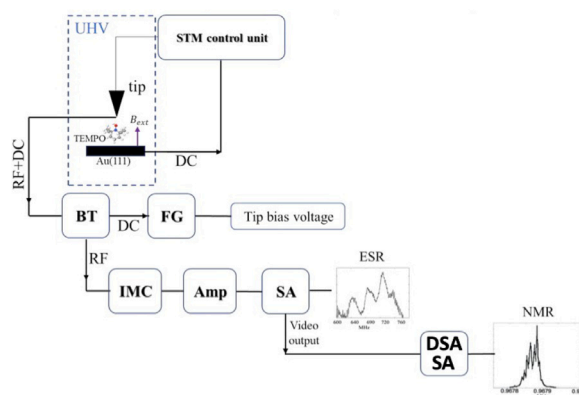


Fig. 6. Setup. NMR-STM acquisition setup.

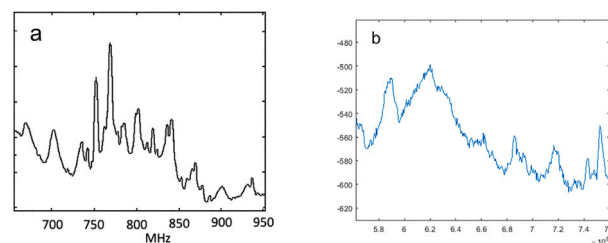


Fig. 7. ESR data on toluene. (a) ESR data with a constant voltage of 2 V, $I = 0.1$ nA, corresponding to $B = 286$ G. (b) ESR data with bias voltage modulation of 0.2 V and 3.8 V at a frequency of 15 MHz, $I = 1$ nA, $B = 235$ G.

The electronic setup for our ESR and NMR data is shown in Fig. 6. DC tunnelling current from the sample was connected to the STM control unit for the STM image acquisition. RF and DC tunnelling currents from the tip were split with a bias-tee (BT) where the DC part (frequency $f < 30$ MHz) was connected to a frequency generator (FG) that modulated the STM tip bias voltage ($0.1 < V_{bias} < 4$ V) with the desired modulation frequency ($0.25 < f < 30$ MHz). The RF part was connected to an impedance matching circuit (IMC) and to an amplifier (Amp). A spectrum analyser (SA) recorded the RF intensity as a function of frequency (span: $200 < f < 800$ MHz) at constant magnetic field, $B_{ext} \approx 230$ G, and the output was the ESR-STM spectrum. Then, the intensity of one of the hyperfine peaks (with a bandwidth of 3 MHz) was digitally recorded and finally its power spectrum calculated (DSA) as a function of frequency, the output was the NMR-STM spectrum.

Fig. 7 shows our ESR-STM spectra on toluene, showing either a constant or a modulated voltage. We note that the distance between the peaks is 17 MHz, as expected for toluene radical anion [25].

We consider next different methods for analysing the time dependent ESR oscillations. In a two stage experiment one spectrum analyser records a chosen hyperfine line intensity as function of time, generating a video output. A second spectrum analyser is directly connected to find the power spectrum of that intensity at the low NMR frequencies (i.e. SA at the bottom of Fig. 6 instead of DSA). The advantage of this method is that a high resolution NMR spectrum is more readily evaluated, the disadvantage is that its spectral resolution is relatively low as seen in Fig. 8a. This method can be improved by a new spectrum analyser with a shorter dwell time.

The results of this procedure are shown at Fig. 8a, the sample is a monolayer of toluene on a gold surface. With $B = 235$ G the NMR signal of ^1H is expected at 1.001 MHz, indeed close to the peak shown in Fig. 8a. We note that the intensity of the NMR peaks are weaker in this method in comparison with the fast scope method, Fig. 2.

We have carried out yet another type of experiment on TEMPO, where the low frequency hyperfine peak intensity in the ESR is analysed

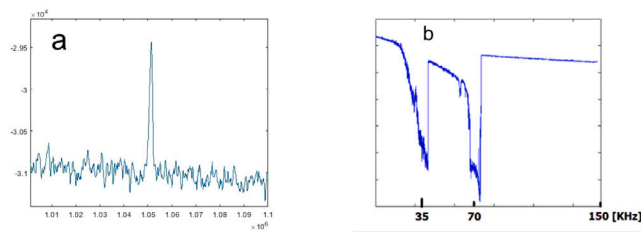


Fig. 8. Additional methods for NMR-STM analysis. (a) Data on toluene: ESR line at 660 MHz is monitored and analysed by a second spectrum analyser. (b) Data on TEMPO: A lock-in method, monitoring the low frequency hyperfine peak. Voltage is modulated between 0.2 V to 3.7 V at a frequency of 250 kHz, $I = 0.1$ nA, $B = 230$ G.

by a lock in amplifier in which the reference frequency was swept from 0 to 150 kHz. A significant signal was detected quite often at 70 kHz, consistent with the Larmor frequency of the ^{14}N nucleus at 230 G (Fig. 8b); an additional signal was observed at half of this frequency. In this experiment a single sweep has taken 90 s, a long time that caused a linewidth much broader than those with the fast scope method, Fig. 4.

We finally summarize the parameters of the experiment, these parameters also appear in the captions of the various figures. The parameters are: Magnetic field B , chosen in the z direction; the STM bias voltage chosen as sample positive (i.e. the tip is at negative voltage with respect to the substrate), if the voltage is modulated with period \bar{T} it has high and low voltage values, each during time $T_1 = T_2 = \bar{T}/2$; the tunnelling current I ; a chosen hyperfine frequency ν_{hyper} that is detected by a spectrum analyser with a bandwidth of 3 MHz; the intensity of this hyperfine signal is detected during a dwell time T_d . We note that $T_d = 0.5 \mu\text{s}$ for the data in Figs. 2, 5 and $T_d = 0.25 \mu\text{s}$ for Figs. 3, 4, for the lock-in method (Fig. 8b) T_d is in some sense its response time $\approx 100 \mu\text{s}$, though this implies a too large $\nu_n T_d$. The second spectrum analyser method (Fig. 8a) acquires time dependent data continuously so T_d is not well defined, indeed the data in Fig. 8a is rather noisy. T_d should be in the range $\nu_n \ll 1/T_d \ll \nu_{\text{hyper}}$ so that ν_{hyper} can be detected accurately (many ESR oscillations within T_d) while the nuclear polarization is almost constant (almost no NMR oscillation within T_d).

Data availability

Data will be made available on request.

References

- [1] H.J. Mamin, M. Poggio, C.L. Degen, D. Rugar, *Nat. Nanotechnol.* 2 (2007) 301–306.
- [2] C.L. Degen, M. Poggio, H.J. Mamin, C.T. Rettner, D. Rugar, *Nanoscale magnetic resonance imaging*, *Proc. Natl Acad. Sci.* 106 (2009) 1313–1317.
- [3] C. Muller, et al., *Nat. Comm.* 5 (2014) 4703.
- [4] M. Pfender, et al., *Nat. Commun.* 10 (2019) 594.
- [5] M. Gulka, D. Wirtitsch, V. Ivády, J. Vodnik, J. Hruby, G. Magchiels, E. Bourgeois1, A. Gali, M. Trupke, M. Nesladek, *Nat. Comm.* 12 (2021) 4421.
- [6] J. Wrachtrup, A. Gruber, L. Fleury, C. von Borczyskowski, *Chem. Phys. Lett.* 267 (1997) 179.
- [7] Y. Manassen, M. Averbukh, M. Jbara, N. Siebenhofer, A. Shnirman, B. Horovitz, *J. Mag. Res.* 289 (2018) 107.
- [8] For a review see, A.V. Balatsky, M. Nishijima, Y. Manassen, *ESR- STM. Adv. Phys.* 61 (2012) 117.
- [9] Y. Manassen, M. Averbukh, M. Morgenstern, *Surf. Sci.* 623 (2014) 47.
- [10] S. Baumann, W. Paul, T. Choi, C.P. Lutz, A. Ardavan, A. Heinrich, *Science* 350 (2015) 417.
- [11] P. Willke, et al., *Sci. Adv.* 4 (2018) eaaq1543.
- [12] J.R. Tolman, K. Ruan, *Chem. Rev.* 106 (2006) 1720–1736.
- [13] Z. Hazan, M. Averbukh, Y. Manassen, *J. Mag. Res.* 348 (2023) 107377.
- [14] url: <https://www.google.com/search?client=firefox-b-d&q=Toluene+NMR#imgsrc=S0bx7852rKbZeM>.
- [15] P. Diehl, H.P. Kellerhals, W. Niederberger, *J. Mag. Res.* 4 (1971) 352.
- [16] W.P. Rothwell, W.X. Shen, J.H. Lunsford, *J. Am. Chem. Soc.* 106 (1984) 2452.
- [17] M. Witanowski, G.A. Webb, *Nitrogen NMR*, Plenum Press, London and NY, 1973.
- [18] Yu-Nian Hsieh, Gerald V. Rubenacker, C.P. Cheng, Theodore L. Brown, *J. Am. Chem. Soc.* 99 (5) (1977) 1384.
- [19] J.A. Jarvis, M. Concistre, I.M. Haies, R.W. Bounds, I. Kuprov, M. Carravetta, P.T.F. Williamson, *Phys. Chem. Chem. Phys.* 21 (2019) 5941.
- [20] Y. Manassen, M. Jbara, M. Averbukh, Z. Hazan, C. Henkel, B. Horovitz, *Phys. Rev. B* 105 (2022) 235438.
- [21] B. Horovitz, A. Shnirman, to be published.
- [22] A. Abragam, B. Bleaney, *Electron Paramagnetic Resonance of Transition Ions*, Clarendon Press, Oxford, 1970.
- [23] B. Horovitz, A. Golub, *Phys. Rev. B* 99 (2019) 241407(R).
- [24] J.E. Wertz, J.R. Bolton, *Electron Spin Resonance Elementary Theory and Practical Applications*, Chapman & Hall, 1986.
- [25] T.R. Tuttle, S.I. Weissman, *J. Am. Chem. Soc.* 80 (1958) 5342.